Contents lists available at ScienceDirect

Journal of Pharmaceutical Analysis

www.elsevier.com/locate/jpa
www.sciencedirect.com

ORIGINAL ARTICLE

LC–UV/MS quality analytics of paediatric artemether formulations

Kirsten Vandercruyssen[a], Matthias D'Hondt[a], Valentijn Vergote[a], Herwig Jansen[b], Christian Burvenich[c], Bart De Spiegeleer[a,*]

[a]Drug Quality and Registration (DruQuaR) group, Faculty of Pharmaceutical Sciences, Ghent University, Harelbekestraat 72, B-9000 Ghent, Belgium
[b]Dafra Pharma International, Slachthuisstraat 30/7, B-2300 Turnhout, Belgium
[c]Department of Physiology and Biometrics, Faculty of Veterinary Medicine, Ghent University, B-9820 Merelbeke, Belgium

Abstract   A highly selective and stability-indicating HPLC-method, combined with appropriate sample preparation steps, is developed for β-artemether assay and profiling of related impurities, including possible degradants, in a complex powder for oral suspension. Following HPLC conditions allowed the required selectivity: a Prevail organic acid (OA) column (250 mm × 4.6 mm, 5 μm), flow rate set at 1.5 mL/min combined with a linear gradient (where $A = 25$ mM phosphate buffer (pH 2.5), and $B =$ acetonitrile) from 30% to 75% B in a runtime of 60 min. Quantitative UV-detection was performed at 210 nm. Acetonitrile was applied as extraction solvent for sample preparation. Using acetonitrile–water mixtures as extraction solvent, a compartmental behaviour by a non-solving excipient-bound fraction and an artemether-solubilising free fraction of solvent was demonstrated, making a mobile phase based extraction not a good choice. Method validation showed that the developed HPLC-method is considered to be suitable for its intended regulatory stability-quality characterisation of β-artemether paediatric formulations. Furthermore, LC–MS on references as well as on stability samples was performed allowing identity confirmation of the β-artemether related impurities. MS-fragmentation scheme of β-artemether and its related substances is proposed, explaining the m/z values of the in-source fragments obtained.

© 2013 Xi'an Jiaotong University. Production and hosting by Elsevier B.V.
Open access under CC BY-NC-ND license.

*Corresponding author. Tel.: +32 9 264 8100; fax: +32 9 264 8193.
  E-mail address: bart.despiegeleer@UGent.be (B. De Spiegeleer).
Peer review under responsibility of Xi'an Jiaotong University.

Production and hosting by Elsevier

1.   Introduction

The past decade has seen an increased interest in specific population targeted and even individualised drug development. Several legislative initiatives in US (*e.g.*, the Best-Pharmaceuticals-for-Children-Act) and Europe (*e.g.*, paediatric investigation plans as indicated in paediatric regulation EC1901/2006), supported by the International Conference of

Harmonisation (ICH) and World Health Organisation (WHO), were recently taken to stimulate and improve the pharmaceutical care-giving to infants, children and adolescents [1–5]. The major challenges encountered are a lack of investigators who are trained in paediatric clinical pharmacology, an inadequate knowledge of drug action mechanisms in a growing child, but foremost a lack of suitable paediatric formulations [6]. It is acknowledged that there is a need for paediatric formulations that permit accurate dosing and enhance patient compliance to significantly reduce child mortality. For oral administration, different types of formulations, aromas and colours may be culture region and age dependent. Different drug concentrations in these various formulations, often at low doses, may also be needed [7]. However, economical constraints limit the development, production and marketing of such paediatric formulations. Up till now, one of the most successful pharmaceutical forms that addresses these specific requirements is undoubtedly the dry powder for oral suspension, due to its ease, robustness and economics of production and distribution, flexible dosing, organoleptic characteristics enhancing the patient acceptability and excellent stability properties. However, the qualitative and quantitative particularities of this dosage form result in different and increased analytical challenges compared to the conventional tablet as most often used for adults.

Half of the world's population is at risk of malaria, and an estimated 216 million cases led to 665 000 deaths worldwide in 2010, of which 91% were in the African Region and about 86% were children under 5 years old. Artemisinin Combination Therapies (ACTs), in which one of the active compounds is a 1,2,4-trioxane derivative like the water soluble artesunate or the lipid soluble β-artemether, are currently recommended by the WHO as first-line treatment for *P. falciparum* malaria. However, access to appropriate treatment is still found to be inadequate due to the relatively high costs of the drugs, combined with insufficient attention to their quality by local health care providers in malaria endemic countries [8].

The full drug potential of artemisinin-derivatives was underestimated in the Western World for many years until very recently, when it has been proven that these 1,2,4-trioxane derivatives possess an anti-parasitic activity in other neglected infections, such as schistosomiasis [9–11] and leishmaniasis [12], as well as an anti-viral activity [13,14]. It has also been confirmed that this group of compounds possesses an important potential as anti-cancer drugs by inducing apoptosis and by inhibiting angiogenesis in different types of tumour cells [15–17]. As a consequence of this awareness, increased research efforts are focused on new derivatives with innovative applications and improved properties. Major pharmaceutical companies are beginning to take an interest in developing new trioxane compounds [18–21].

Current analytical techniques describe derivatisation-based methods [22], gas chromatography (GC) [23], thin layer chromatography (TLC) [24], supercritical fluid chromatography (SCFC) [25], spectroscopic [26] and immunological techniques [27,28], but it is clear that the main-stream methods are mainly based on high performance liquid chromatography (HPLC), coupled to ultra violet (UV), evaporative light scattering detector (ELSD), electron capture detection (ECD) or electrospray ionisation (ESI)–mass spectrometry (MS) detection [29–32]. Up till now, the focus was directed to biological matrices like plasma for pharmacokinetic information [33,34], to plant derived samples for production reasons [23,35,36] or for environmental eco-toxicity studies [37,38]. However, with the advent of a plethora of newly developed 1,2,4-trioxane derivatives and the urgent demand to develop suitable paediatric formulations, there is a clear need for analytical methods which are suitable for quality purposes for finished

drug products (FDP). The availability of suitable quality methods is currently also one of the key issues in the efficient regulatory approval for clinical trials and marketing. These methods should encompass not only the assay of the active pharmaceutical ingredient (API) in FDP's as up till now described [39–42] but also more importantly they should focus on all related compounds, including the possible degradants, respecting the pharmaceutically low specification limits. Recently, an impurity evaluation of artemisinin, the plant-derived starting material for API-production (*e.g.*, β-artemether and artesunate) was reported [43,44]. In addition, our research group has developed a new approach for the calculation of the relative response factors of β-artemether degradants, using dry heat stress, under various time, temperature and environmental conditions, thus solving the peak area/mass balance question [45].

The aim of this study was to investigate two specific analytical challenges related to low-artemether-dosed, high-bulk-containing paediatric powders for oral suspension (180 mg/60 mL after reconstitution in water), *i.e.*, (1) sample preparation, where the extraction solvent interacts with the excipients, and (2) the chromatographic characterisation of a new, highly selective HPLC system allowing separation of artemether-related impurities and excipients. Furthermore, LC–MS on stability samples of the powders for oral suspension stored for 6 months at 40 °C/75% relative humidity (RH), supported the selectivity of the method, indicating multiple degradants at low concentrations. Finally, an in-source fragmentation pathway for β-artemether and its related substances, explaining the observed *m/z* values, is proposed.

2. Materials and methods

2.1. Materials

The developmental FDP's, a powder for oral paediatric suspension, were gifts from Dafra (Turnhout, Belgium) and consisted of β-artemether (0.7%, m/m), lumefantrine (4.5%, m/m), saccharose, cellulose, gums, parabens, silica, acidifying and flavouring agents. The individual constituents of the formulation, including lumefantrine, as well as the related 1,2,4-trioxane compounds artesunate, dihydroartemisinin (DHA), artemisinin, 9,10-anhydroartemisinin (AHA), and α-artemether, were obtained from Dafra (Turnhout, Belgium). From Sigma Tau (Rome, Italy), the degradation compound 2-[4-methyl-2-oxo-3-(3-oxobutyl)cyclohexyl]propanal (DKA) was acquired. HPLC gradient grade acetonitrile was purchased from Fisher Scientific (Leicestershire, UK), hydrochloric acid from UCB (Leuven, Belgium) and potassium dihydrogen phosphate from Merck (Darmstadt, Germany). Water was purified using an Arium 611 purification system (Sartorius, Göttingen, Germany) to laboratory-graded water (18.2 M Ω cm).

2.2. HPLC-PDA system

The HPLC-photodiode array (PDA) apparatus consisted of a Waters Alliance 2695 separations module and a Waters 2996 PDA detector with Empower 2 software for data acquisition (all Waters, Milford, MA, USA). HPLC-analysis was performed using a Prevail organic acid (OA) column (250 mm × 4.6 mm, 5 μm) with guard column (7.5 mm × 4.6 mm, 5 μm) (Grace-Alltech, Deerfield, IL, USA) thermostated at 25 °C. The flow rate was set at 1.5 mL/min and linear gradient was applied (where $A = 25$ mM phosphate buffer, adjusted to pH 2.5 with diluted hydrochloric acid, and $B =$ acetonitrile), running from 30% to 75% B

from 0 to 60 min, followed by returning to the initial conditions and re-equilibration. The sample compartment was maintained at 5 °C and the injection volume was 20 μL. The UV-spectrum was recorded between 190 and 400 nm, with 210 nm as the representative wavelength for quantification.

2.3. HPLC–MS system

The LC–UV/MS apparatus consisted of a Spectra System SN400 interface, a Spectra System SCM1000 degasser, a Spectra System P1000XR pump, a Spectra System AS3000 autosampler and a Finnigan MAT LCQ mass spectrometer (all Thermo, San Jose, CA, USA), equipped with an SPD-10A UV–vis detector at 210 nm (Shimadzu, Kyoto, Japan) and software Xcalibur 1.2 software (Thermo) for data acquisition. For the MS-experiments described in this paper, the samples were loaded onto a Prevail OA column (250 mm × 4.6 mm, 5 μm) with guard column (7.5 mm × 4.6 mm, 5 μm) (Grace-Alltech, Deerfield, IL, USA), both thermostated at 25 °C. An adaptation was made of the mobile phase towards ESI-MS compatibility, i.e., replacing the phosphate buffer pH 2.5 by 0.1% (m/v) formic acid. The same linear gradient elution was performed at a flow rate of 1.5 mL/min. The sample compartment was maintained at 5 °C and the injection volume was 20 μL. Electrospray was using nitrogen sheath gas (90 arb, corresponds to 1.35 mL/min) and auxillary gas (30 arb, corresponds to 0.45 mL/min) in positive ionisation mode (m/z 100–500). The capillary voltage was set at +4 kV, combined with a capillary temperature of 230 °C.

2.4. GC-FID system

The acetonitrile content in the development experiments of the extraction procedure was assayed using a high throughput GC-Flame Ionisation Detector (FID) method. The GC apparatus consisted of a separation module provided with an FID controlled by TotalChrom Navigator (all Perkin Elmer, Massachusetts, USA). GC separations were performed using a Glass column (2 m × 3 mm) packed with 10% Carbowax 20 M on Chromosorb G thermostated in an oven set at 120 °C. Injector and detector temperatures were both 250 °C. Nitrogen was used as a carrier gas at a flow rate of 20 mL/min. The injection volume was 2 μL (split, 1:50) and ethanol was used as internal standard.

2.5. Sample preparation

2.5.1. Solvent composition for extraction
Acetonitrile–water mixtures with different concentrations of water (40–0%) were tested to explore the influence on artemether recovery. During development of the extraction procedure, artemether-test, spiked placebo and reference solutions were prepared with the different solvent compositions. The final choice for the extraction solvent was pure acetonitrile.

2.5.2. Reference solutions
Reference solutions for validation and quantification of β-artemether and related substances were prepared by dissolving the reference substances in acetonitrile. Solutions were produced containing β-artemether at 120%, 110%, 100% (i.e., approximately 3.5 mg/mL), 90% and 80%. In addition, at lower concentrations, dihydroartemisinin at 6%, 5%, 4%, 3% and 2% label claim (% l.c.). and the other related substances (artemisinin and α-artemether) at

0.30%, 0.25%, 0.20%, 0.15% and 0.10% l.c., whereby 100% l.c. corresponded to the label claim of β-artemether, were dissolved.

2.5.3. Artemether-test solutions of paediatric powder
Test solutions for artemether assay were prepared by extracting 4.400 g of finished drug product with 10.0 mL of acetonitrile. After shaking for 30 min and sonication for 15 min, it was centrifuged for 5 min at 4555 g at room temperature. Finally the supernatant was filtered through a 0.45 μm regenerated cellulose filter (Whatman®), discarding the first 2 mL of filtrate. For quantification of related degradants and impurities, reconcentrated solutions were prepared by taking 1.0 mL of the test solution followed by evaporation using a gentle stream of nitrogen and redissolving in 100 μL of acetonitrile.

2.5.4. Artemether-spiked solutions of placebo powder
Spiked placebo solutions were prepared as described for the test solutions, replacing the extraction solvent by 10.0 mL of the corresponding reference solution (see Section 2.5.2). The placebo powder for a 60 mL suspension after reconstitution in water consists of 4.77% lumefantrine, 86.33% saccharose, 5.96% microcrystalline cellulose, 0.26% citric acid monohydrate, 0.53% xanthan gum, 0.21% methyl paraben, 0.05% propyl paraben, 0.79% coconut flavour and 0.30% colloidal anhydrous silica (all in m/m). Reconcentrated solutions were prepared in the same manner as previously described (see Section 2.5.3).

2.5.5. Solutions for GC analysis
Ethanol (10%, v/v in water) was selected as the internal standard. Reference solutions were prepared by transferring approximately 70 mL of water into a 100.0 mL volumetric flask, followed by addition of 1000 μL extraction solvent, varying from 60% to 100% acetonitrile content and 10.0 mL of internal standard solution, followed by immediately dilution to volume with water. Test solutions of each spiked placebo extract (varying from 60% to 100% acetonitrile) were prepared in the same manner.

2.5.6. Solutions for LC–MS analysis
Spiked placebo solutions were prepared containing the related compounds diketoaldehyde (DKA), dihydroartemisinin (DHA), α-artemether, 9,10-anhydroartemisinin (AHA) and artemisinin at approximate concentrations of 17.5 μg/mL, which is equivalent to 0.5% of β-artemether l.c. Co-artesiane stability samples, stored for 6 months at 40 °C and 75% RH (accelerated ICH conditions), were prepared by the same extraction procedure (see Section 2.5.3).

2.6. Validation

Method validation was performed using the spiked placebo solutions and reference solutions for the β-artemether assay. Reconcentrated solutions of spiked placebo and reference solutions were applied for the validation of the determination of β-artemether-related substances in the paediatric powder for oral suspension. Accuracy, precision and linearity were evaluated for all determinations.

3. Results

3.1. Development of extraction procedure

As low UV-detection (*i.e.,* 210 nm) is used, methanol, tetrahydrofuran (THF) and chloroform mixtures as organic solvent component as extraction solvent were excluded and acetonitrile, with its low UV cut-off value of 190 nm, was retained. Moreover, initial sample preparation experiments using chloroform-based solvents [39] showed generally significant peak broadening, negatively influencing the separation of closely eluting related impurities. As it is a common practice in pharmaceutical sample processing to use aqueous-based organic extraction solvents for better compatibility with the reversed-phase chromatographic system, we investigated the aqueous-acetonitrile based extraction. This type of extraction solvent for β-artemether is also recommended in the International Pharmacopoeia monograph 'artemether injection' [46], completely dissolving fractionated coconut oil or the medium chain triglycerides oil (which are used in FDP like Artesiane), while with arachis oil (used in *e.g.,* Mantera), resulting in a two-phase extraction and separation. Other solvents such as THF and isopropanol yielded always a one-phase system, independent of the oil-type used. However, THF is quite volatile and unstable, making its handling more problematic and thus not an ideal solvent for sample preparation. While isopropanol was a good solvent for the oil preparations and in the extraction of the powder, it gave a more pronounced unretained signal, thereby increasing the risk of masking polar degradants of β-artemether. Therefore, the optimisation of the extraction procedure was performed with acetonitrile–water based sample solvents.

A non-linear relationship was found between the β-artemether recovery and percentage acetonitrile in the extraction solvent, decreasing from 167% to 101% recovery for an acetonitrile content varying from 60% to 100%, respectively (Fig. 1). The recovery-increasing effect due to solvent composition was not observed for extraction solvent compositions with 10% water or less. To investigate if and to what extent the solvent composition influenced the chromatographic behaviour of the β-artemether peak, the symmetry factors and plate counts as described by the Ph. Eur. were calculated: no significant effects were observed under our operational conditions. It was thus hypothesised that the water in the extraction solvent was bound onto the FDP matrix, leading to an acetonitrile-enriched supernatant liquid, which contains nearly all β-artemether present in the sample. Based on
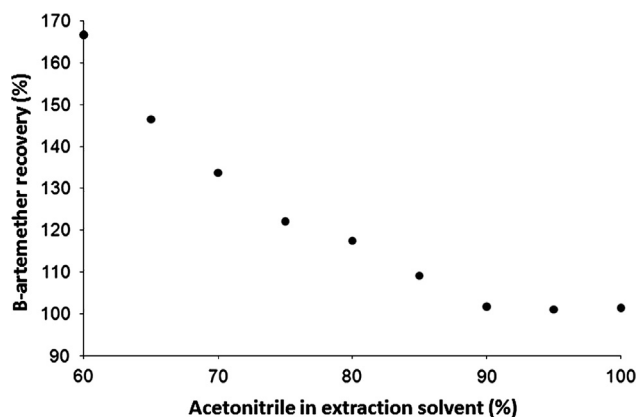
this hypothesis, β-artemether recovery was calculated assuming only acetonitrile as the dissolving liquid (Table 1). The lower recoveries calculated for acetonitrile indicate that not all water in the extraction solvent is bound to the excipients, and hence that the

Table 1 β-Artemether recoveries.

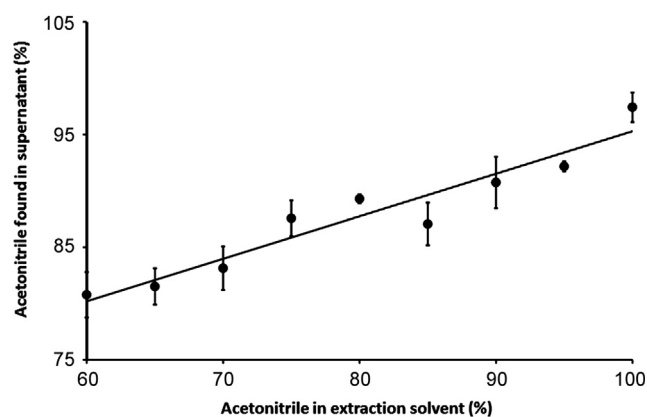| #	ACN in extraction solvent (%)	β-Artemether recovery (%)	β-Artemether recovery ACN-only (%)
A	60	166.7	100.0
B	65	146.5	95.2
C	70	133.7	93.6
D	75	122.0	91.5
E	80	117.4	93.9
F	85	109.1	92.7
G	90	101.7	91.5
H	95	101.0	96.0
I	100	101.4	101.4

Fig. 2 Percentage acetonitrile found in the test solutions (given as means with 95% confidence intervals) in function of percentage acetonitrile in the extraction solvent.
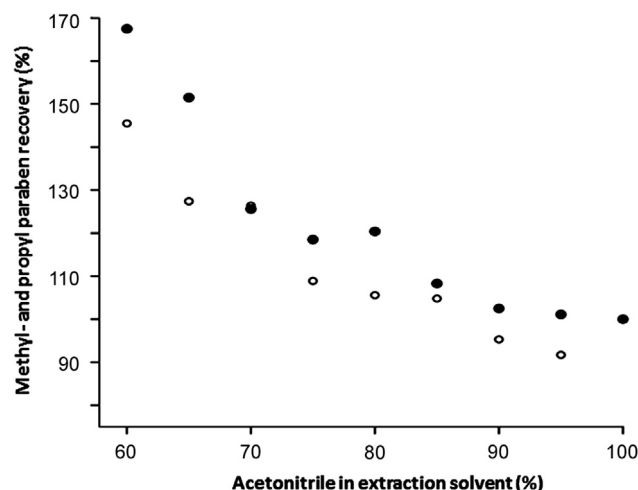

Fig. 1 β-Artemether recovery in function of percentage acetonitrile in the extraction solvent.

Fig. 3 Methyl- (○) and propyl- (●) paraben recovery in function of percentage acetonitrile in the extraction solvent.

freely available solvent (after extraction) still contains some water. Further investigation on the exact composition of the supernatant after extraction of the FDP was thus performed using GC-analysis. A graph showing the percentage acetonitrile found in the supernatant test solutions in function of the theoretical acetonitrile concentration (*i.e.*, exact composition of extraction solvent before being added to
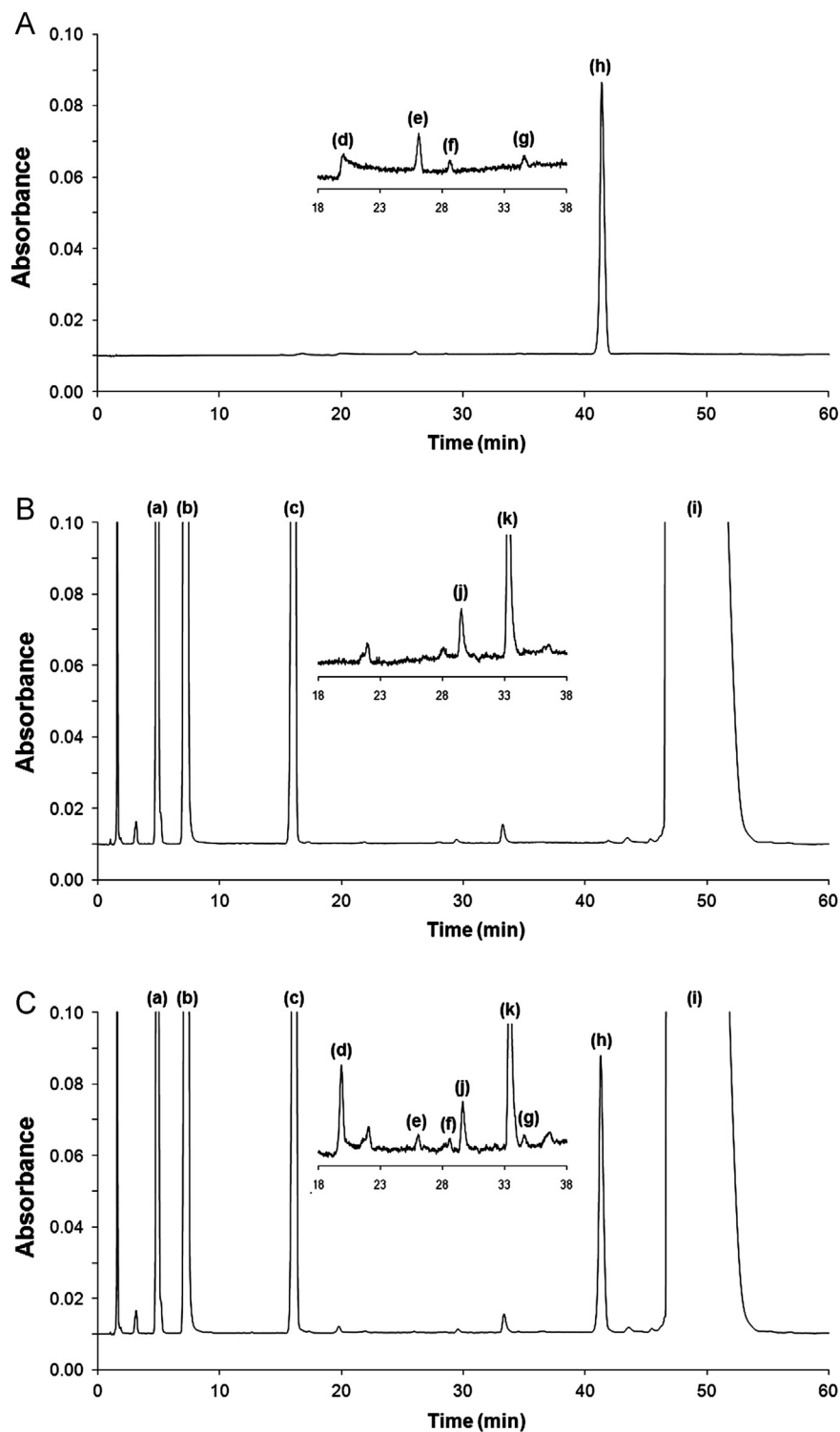

Fig. 4 Typical chromatograms (UV at 210 nm) showing reference solution (A), placebo solution (B) and spiked placebo solution (C) obtained on the Prevail OA column using the chromatographic conditions as described in the experimental section. Peak identities are as follows: (a) coconut flavour, (b) methyl paraben, (c) propyl paraben, (d) α-dihydroartemisinin, (e) β-dihydroartemisinin, (f) artemisinin, (g) α-artemether, (h) β-artemether, and (i) lumefantrine. Peaks (j) and (k) were identified as lumefantrine-related impurity degradants.

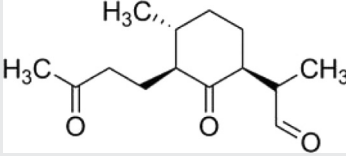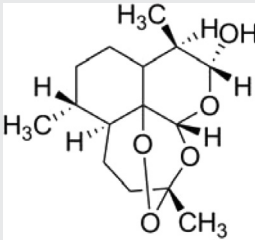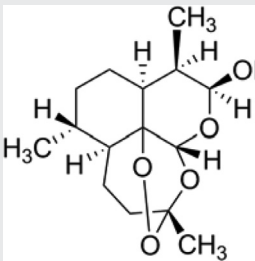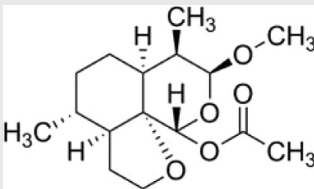**Table 2** Overview of general information on β-artemether and related compounds: RRT HPLC *vs.* RRT MS.
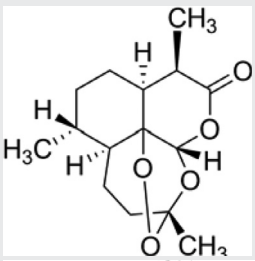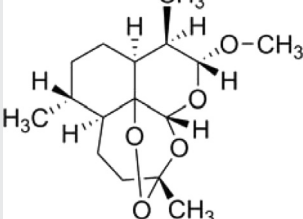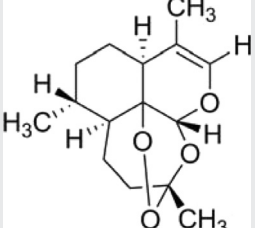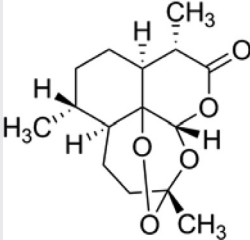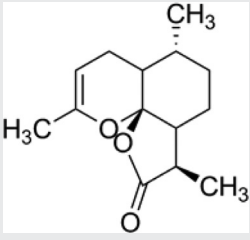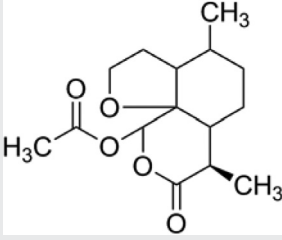
#	Chemical name	Structure	RRT HPLC	RRT MS	RRF[a]
1	**Diketo aldehyde (DKA)** 2-[4-Methyl-2-oxo-3-(3-oxobutyl) cyclohexyl]propanal [$C_{14}H_{22}O_3$, 238.32] [62,63]		0.41	0.40	3.41
2	**α-Dihydroartemisinin** (3R,5aS,6R,8aS,10S,12R,12aR)-Decahydro-10-hydroxy-3, 6,9-trimethyl-3,12-epoxy-12H-pyrano[4.3-j]-1,2-benzodioxepin [$C_{15}H_{24}O_5$, 284.35] [53]		0.48	0.50	1.08
3	**β-Dihydroartemisinin** (3R,5aS,6R,8aS,10S,12R,12aR)-Decahydro-10-hydroxy-3,6,9-trimethyl-3,12-epoxy-12H-pyrano[4,3-j]-1,2-benzodioxepin [$C_{15}H_{24}O_5$, 284.35] [53,64]		0.64	0.65	1.08
4	**Furano acetate** (3aS,4R,6aS,7R,8S,10R,10aR)-8-Methoxy-4,7-dimethyloctahydro-2H-furo[3,2-i][2]benzopyran-10-yl acetate [$C_{16}H_{26}O_5$, 298.37] [65]		0.69	0.69	n.a.
5	**Artemisinin** (3R,5aS,6R,8aS,9R,12S,12aR)-Octahydro-3,6,9-trimethyl-3,12-epoxy-12H-pyrano[4,3-j]-1,2-benzodioxepin-10(3H)-one [$C_{15}H_{22}O_5$, 282.33] [66]		0.71	0.71	1.10
6	**α-Artemether** (3R,5aS,6R,8aS,10R,12R,12aR)-Decahydro-10-methoxy-3,6,9-trimethyl-3,12-epoxy-12H-pyrano[4,3-j]-1,2-benzodioxepin [$C_{16}H_{26}O_5$, 298.37] [64,67]		0.85	0.83	1.03
7	**9,10-Anhydroartemisinin (AHA)** (9,10-Anhydro-10-deoxoartemisinin) [$C_{15}H_{22}O_4$, 266.33] [68]		0.91	0.91	21.30

Table 2 (*continued*)

#	Chemical name	Structure	RRT HPLC	RRT MS	RRF[a]
8	**β-Artemether** (3*R*,5a*S*,6*R*,8a*S*,9*R*,10*S*,12*R*,12a*R*)-Decahydro-10-methoxy-3,6,9-trimethyl-3,12-epoxy-12H-pyrano [4,3-*j*]-1,2-benzodioxepin [$C_{16}H_{26}O_5$, 298.37] [69]		1.00	1.00	1.0
9	**9-Epi-artemisinin** (1*R*,5*R*,12*S*)-1,5,9-Trimethyl-11, 14,15,16-tetraoxatetracyclo-hexadecan-10-one [$C_{15}H_{22}O_5$, 282.33] [44]		n.a.	n.a.	1.37
10	**Artemisitene** 3,12-Epoxy-12*H*-pyrano[4,3-*j*]-1,2-benzodioxepin-10(3H)-one,octahydro-3,6-dimethyl-9-methylene-(3*R*,5a*S*,6*R*,8a*S*,12*S*,12a*R*) [$C_{15}H_{20}O_5$, 280.13] [44,70,71]		n.a.	n.a.	37.52
11	**Deoxyartemisinin** (1*R*,9*R*)-1,5,9-Trimethyl-11,14,15-trioxatetracyclo-pentadecan-10-one [$C_{15}H_{22}O_4$, 266.33] [70,72]		n.a.	n.a.	n.a
12	**Artemisinic acid** 2-(7-Methyl-1,2,3,4,4a,5,6,8a-octahydronaphthalen-1-yl)prop-2-enoic acid [$C_{14}H_{20}O_2$, 220.31] [43,70]		n.a.	n.a.	n.a
13	**Arteannuin B** (1a*R*,1b*R*,4a*S*,7*R*,7a*S*,9a*R*)-7,9a-Dimethyl-4-methylenedecahydro-3H-oxireno[7,8]naphtho[8a,1-b]furan-3-one [$C_{15}H_{20}O_3$, 248.32] [43,73]		n.a.	n.a.	n.a

Table 2 (*continued*)

#	Chemical name	Structure	RRT HPLC	RRT MS	RRF[a]
14	**Proposed structure of major artemisinin impurity** (3*R*,5a*S*,6*R*,8a*S*,9*R*,12*S*,12a*R*)-Octahydro-3,6,9-trimethyl-3,12-epoxy-12*H*-pyrano[4,3-*j*]-1,2-benzodioxepin-10(3*H*)-one [$C_{15}H_{22}O_5$, 282.33] [43]		n.a.	n.a.	n.a
15	**Proposed structure of artemisinin degradant** (3*R*,6*R*,10a*S*)-3,6,9-Trimethyl-3a,4,5,6,6a,7-hexahydrofuro[3,2-*i*]chromen-2(3*H*)-one [$C_{14}H_{20}O_3$, 236.31] [43]		n.a.	n.a.	n.a
16	**Proposed structure of artemisinin degradant** (7*R*)-4,7-Dimethyl-8-oxooctahydro-2*H*-furo[3,2-*i*]isochromen-10-yl acetate [$C_{15}H_{22}O_5$, 282.33] [43]		n.a.	n.a.	n.a

n.a. not applicable
[a]RRF or relative response factors calculated by our research group [45].

powder) is given in Fig. 2. From above data, the recovery-extraction solvent relationship may at least be partly explained as a dehydration of the extraction solvent. For instance, acetonitrile–water 60:40%, (v/v) as extraction solvent being dehydrated to acetonitrile–water 80:20% (v/v) (see Fig. 2) would theoretically yield 133% recovery. However, this still contrasts the actual 167% recovery found for β-artemether. Therefore, also a part of acetonitrile is included in the non-solving (β-artemether-free) solvent fraction bound to the powder particles.

To further verify our bound/free solvent hypothesis, effects of the solvent composition on methyl and propyl paraben recoveries were verified using the spiked placebo solutions and the results obtained for these two preservatives are shown in Fig. 3. Similar extraction solvent dependent effects were observed for the recovery of the two preservatives as for β-artemether, although less pronounced for methyl paraben (log $P \approx 1.9$ *vs.* 2.90 and 2.82 for propyl paraben and β-artemether, respectively [47]). This indicates that the major effect is the free-bound solvent volume change, where the water is the dominant solvent component, but that the physico-chemical properties of the compound itself (*e.g.,* solubility in different aqueous-acetonitrile mixtures) also play a role. By overall results of the several tests, selection of 100% acetonitrile as extraction solvent is made.

3.2. HPLC-method for determination of β-artemether and related substances

3.2.1. Selectivity
Several HPLC columns, *e.g.*, Purospher Star RP-18e, LiChrospher 100 RP-18, Microsorb 100C$_{18}$) were previously tested for their selectivity. However, the best overall selectivity was obtained with a new column, *i.e.,* the Prevail OA column, which is a specific type of polar-embedded reversed-phase stationary phase. The excellent selectivity performance of this Prevail OA method for the analysis of 1,2,4-trioxane derivatives is demonstrated by typical chromatograms of the β-artemether-containing FDP given in Fig. 4. Selectivity was demonstrated by the retention characteristics of the placebo-excipient chromatograms, structurally related compounds (*e.g.,* artesunate) and related impurities including potentially present degradants (*i.e.,* α-artemether, DHA and DKA), and possible other API (*e.g.,* lumefantrine) and its degradants (*e.g.*, desbenzylketo lumefantrine derivative) [48]. Even in the presence of extremely large peaks from other ingredients, such as flavouring agent, preservatives and lumefantrine (with peak areas being 3–84 times that of β-artemether), β-artemether and its related compounds at low concentrations can still be unequivocally determined without interference from these drug product

Table 3 Method validation results.

Validation attribute	β-Artemether	DHA	Artemisinin	α-Artemether
	90–120% l.c. (n=6)	2–6% l.c. (n=3)	0.1–0.3% l.c. (n=3)	0.1–0.3% l.c. n=3
Accuracy (recovery) (%)	99.9	96.5	105.2	106.0
Precision (R.S.D.) (%)	0.43	6.68	6.52	8.27
Linearity				
Intercept (95% C.I.) (µAU s)	−99 340 to 161 126	−406 463 to 244 612	191 to 8479	−10 885 to 20 699
Slope (95% C.I.) (µAU s/% l.c.)	18 141 to 20 735	134 116 to 284 810	177 512 to 215 878	128 482 to 274 688
R^2	0.9977	0.9992	0.9999	0.9992
Quantification limit (µg/mL)[a]	5.5 (0.31% l.c.)	11.48 (0.33% l.c.)	3.9 (0.11% l.c.)	4.7 (0.13% l.c.)

[a] Calculated as $S/N=10$ (Ph. Eur.).

ingredients. Under our conditions, β-artemether was eluted at approximately 40 min, while the more hydrophilic DKA, artesunate and 9,10-anhydroartemisinin (AHA) were sufficiently retained at 17, 24 and 37 min, respectively (Table 2). The elution times of the other compounds were: 20 and 26 min (DHA epimers), 28 min (artemisinin) and 34 min (α-artemether). No interference was seen with the early eluting excipients, including parabens, lumefantrine and the different aroma-compounds. While this method is considerably longer than the previously published methods, its selectivity is demonstrated to be significantly higher, allowing the individual determination of β-artemether related impurities including degradants. This was not possible with the existing shorter and isocratic methods. Moreover, stress degradation under various conditions, i.e., HCl, NaOH and H_2O_2 as well as dry heat conditions, resulted in additional peaks, which are clearly separated from β-artemether. This stress degradation study (see Supplementary information) served to demonstrate the high selectivity of the HPLC-methodology, as well as to draw attention to possible degradation-peaks, which can be looked after in the ICH accelerated and long-term stability studies. It is noted that although UV-DAD peak purities higher than 99.0% were obtained on the β-artemether peaks in the samples, this was not considered as an ultimate proof of specificity, seen the rather non-specific UV spectra of these trioxane derivatives.

3.2.2. Validation
Validation of our final method resulted in the performance characteristics as summarised in Table 3. The specified, identified degradants of β-artemether in the FDP currently include α- and β-DHA epimers, α-artemether and artemisinin. A linear correlation was found between the peak areas and the concentrations in the assayed range of β-artemether and its identified degradants. For all compounds the regression coefficients (R^2) were greater than 0.995, demonstrating the linearity of the method. For the β-artemether-assay, spiked placebo solutions (n=6) were investigated for precision and accuracy, resulting in a RSD-value less than 2.5% and a recovery to be within 95.0–105.0%. Reconcentrated spiked placebo solutions were also analysed for precision and accuracy for the determination of the other related compounds. For DHA, α-artemether and artemisinin, respectively, a mean RSD-value of 7.16% and a recovery of 102.6% were found. From these data, the developed HPLC-method for the determination of β-artemether and its related substances in paediatric powder for oral suspension, is considered to be suitable for its intended purpose, i.e., regulatory quality analysis of samples from ICH long-term and accelerated stability studies.

3.3. LC–MS characterisation

Similar chromatographic retention times were obtained using the modified mobile phase, i.e., 0.1% (m/v) formic acid for ESI-MS compatibility (Table 2). The full scan mass spectra (m/z 100–500) acquired for β-artemether (m/z 299) and artemisinin (m/z 283) are given in Fig. 5, while Table 4 gives an overview of the MS data of β-artemether, artemisinin and their identified related substances. The in-source fragmentation pathways for artemether and artemisinin are proposed in Figs. 6 and 7, respectively.

3.3.1. β-artemether
For β-artemether, the following qualifier ions are withheld: m/z 267, m/z 249, m/z 239, m/z 221 and m/z 163. Due to in-source fragmentation, the protonated form or parent ion of β-artemether $[M+H]^+$ with m/z of 299 is not detected. Our fragmentation process was considered to consist of following steps: m/z 267 $[M+H–CH_3OH]^+$ as $[AHA+H]^+$, m/z 249 $[M+H–CH_3OH–H_2O]^+$, m/z 239 $[M+H–CH_3OH–CO]^+$ as $[DKA+H]^+$, m/z 221 $[M+H–CH_3OH–CO–H_2O]^+$ and m/z 163 $[M+H–CH_3OH–CO–H_2O–C_3H_6O]^+$ (Fig. 6). The ion m/z 281 $[M+H–H_2O]^+$ is also observed, explained by elimination of water from the protonated β-artemether.

3.3.2. Artemisinin
For artemisinin, the predominated peaks observed are m/z 283 (corresponding to the parent ion $[M+H]^+$), m/z 265, m/z 248, m/z 237, m/z 219, m/z 209, m/z 191 and m/z 163. The m/z 145 is reported above the reporting cut-off threshold (20% relative abundance) with artemether and AHA, but is not observed as a significant fragment in artemisinin. Due to its very characteristic m/z values, artemisinin is expected to follow another fragmentation pathway, different from β-artemether and its related impurities, DHA, AHA and DKA. Following steps in the in-source fragmentation pathway of artemisinin are proposed: m/z 265 $[M+H–H_2O]^+$ and m/z 237 $[M+H–H_2O–CO]^+$ (Fig. 7).
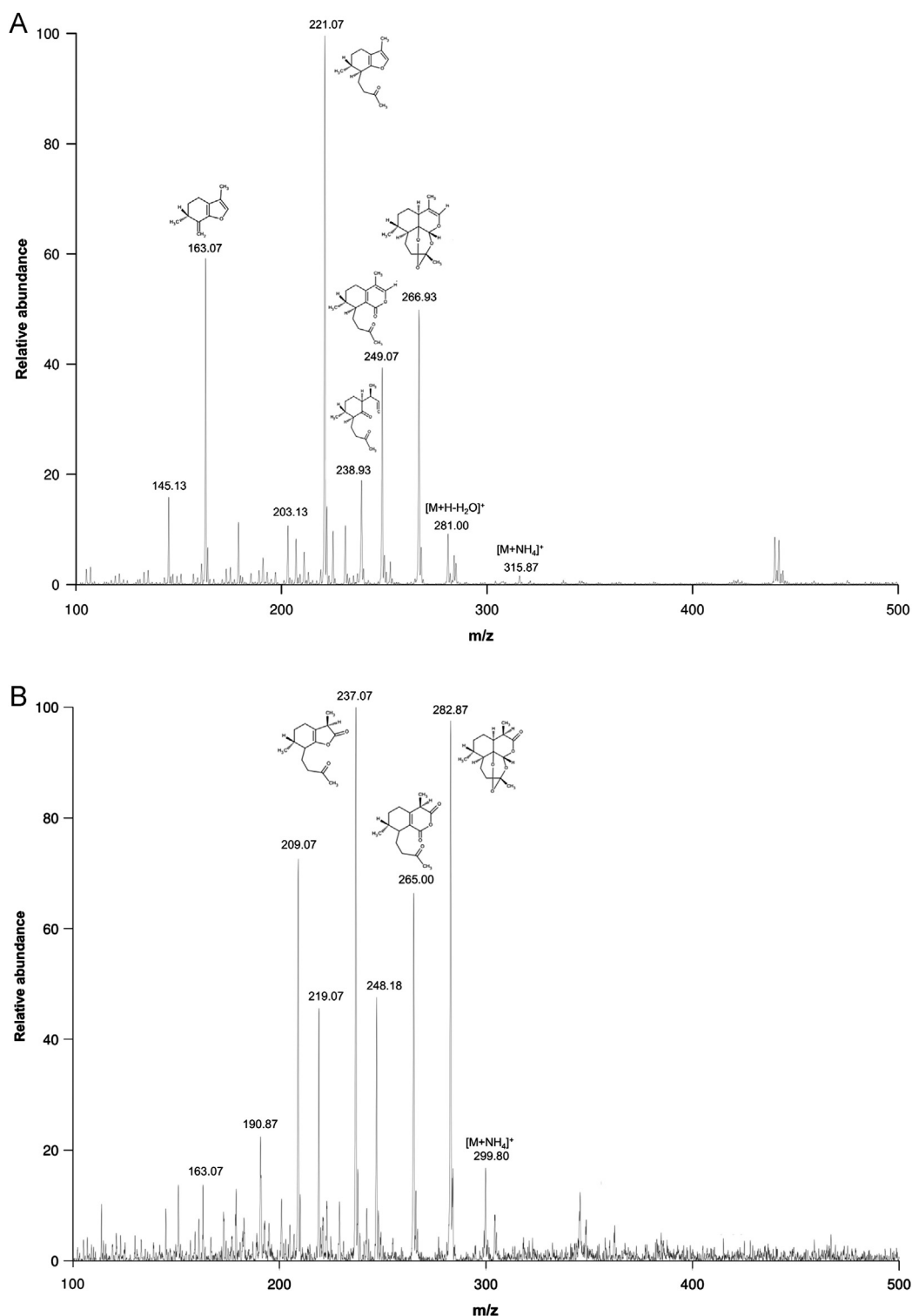
Fig. 5 Mass spectra of β-artemether (A) and artemisinin (B), together with structures allocated to the in-source fragments.

4. Discussion

It is well-known that volumes of solution formation are not additive, *i.e.*, volume change is not conserved under the process of solution formation, because the intermolecular forces of a mixture are different from these forces in the pure substances. This property is expressed by the partial molar volume, which is the change in volume per mole compound added to a specific solvent under defined temperature and pressure. Simple systems like acetonitrile solutions in water have been investigated, and a partial molar volume of around 45 mL/mol acetonitrile (at 298.15 K and 1 atm) has recently been calculated [49]. The partial molar volume of solids is also a topic of current physico-chemistry research. Nevertheless, in pharmaceutical analysis, the concept of the

Table 4 MS spectra of β-artemether and related substances.

Peaks (mz) observed[a]	Compound							
	DKA-related	DKA	α-DHA	β-DHA	Artemisinin	α-Artemether	AHA	β-Artemether
113.9	–	–	–	+	+	–	+	–
145.1	–	–	–	–	–	+	+	+
163.1	+	+	++	++	+	++	+	+
182.4	–	–	–	+	–	–	–	–
190.9	–	–	–	+	+	–	+	–
192.8	–	–	–	+	–	–	–	–
207.1	–	–	–	–	–	+	+	–
209.3	–	–	–	–	+	–	–	–
219.0	–	–	–	–	+	–	–	–
221.1	++	++	++	++	–	+	++	++
224.7	–	–	–	–	–	–	+	–
230.3	–	–	–	–	–	+	+	+
237.0	–	–	–	–	++	–	–	–
238.9	+	+	+	+	–	+	+	+
241.5	–	–	–	–	–	–	+	–
242.3	–	–	+	+	–	–	–	–
246.1	–	–	–	–	+	–	–	–
249.0	–	–	+	+	–	+	++	+
265.1	–	–	–	–	++	–	–	–
266.8	–	–	+	+	–	+	++	+
282.9	–	–	–	–	++	–	–	–
283.9	–	–	–	–	–	+	–	–
315.8	–	–	–	–	–	++	–	+

[a]Reporting threshold: 20% relative abundance.

partial molar volume is normally not of any concern, due to the volumetric handling of liquid mixtures as extraction solvents, together with a low quantity of excipients, which are moreover often insoluble in the extraction solvent. However, these and other solvent volume effects are no longer negligible in paediatric formulations, which are currently being developed under regulatory supportive actions: they contain substantial amounts of excipients compared to the API-quantity for dosing and child-acceptability reasons. These high-bulk excipients are often mixtures of soluble and insoluble compounds in the analytical extraction solvents. Consequently, in these cases, the final solvent volume needs careful attention in quantitative analysis. First of all, the dissolution of appreciable quantities of excipients like sucrose will also influence the final volume: for simple aqueous sucrose solutions, a partial molar volume of around 300 mL/mol sucrose was recently determined, exhibiting an hydration number of around 5, equivalent to approximately 10% water bound in similar situations as in our case, leaving 90% of the water volume free [50]. However, our analytical situation is more complex, as the extraction solvent is a mixture of acetonitrile and water, and the powder does consist not only of sucrose but of other soluble and insoluble components as well. Our data indicate a more complex "2-compartmental" solvent distribution, i.e., a free (available) and a bound (unavailable) solvent fraction, which cannot completely be explained alone by the partial molar volume data currently available. There is a preferential, but not complete, binding of water to the excipients: some water is still present in the freely available fraction and some acetonitrile is present in the bound-unavailable solvent fraction as well. There is an initial exchange of excipient-bound water with pure acetonitrile, up to 10% water in

the extraction solvent, which keeps the freely available extraction solvent constant. At increasing water content (above 10%) in the extraction solvent, the volume of free solvent decreases. Moreover, also the analyte itself plays an analytically relevant role, depending on its physico-chemical solubility and hydrophobicity characteristics. This is consistent with a recent explanation of concentration-distance water-bound gradient from colloid surfaces [51]. It is clear that small changes in extraction solvent composition used in the analysis of paediatric formulations have major consequences.

The Prevail OA column was recently specifically designed and up till now only used for the analysis of organic acids. Its proprietary silica-based polar-embedded bonding chemistry enables the use of highly aqueous eluents without stationary-phase dewetting. Compared to other RP columns previously used in the analysis of 1,2,4-trioxane derivatives, this column showed a significant improvement in chromatographic performance compared to those previously described and tested by us, i.e., Purospher Star, LiChrospher, Microsorb. A recently reported method was only partly suitable for the assay, characterised by very high asymmetry factors according to regulatory pharmacopoeial criteria, and did not report any related compound [39]. Using the Prevail OA column, dihydroartemisinin (DHA) did show on-column epimerisation into its α- and β-form as recently reported for other columns as well [52,53]. It was found that other components in the analytical aliquot influenced this behaviour, as demonstrated in Fig. 4: the chromatograms of a pure acetonitrile reference solution (Fig. 4A) showed significant on-column epimerisation whilst this was not observed with a sample solution (Fig. 4C). This warrants careful interpretation in the methodology development, as not only the aging of the column but also the composition of the analytical solutions will influence this epimerization behaviour. When
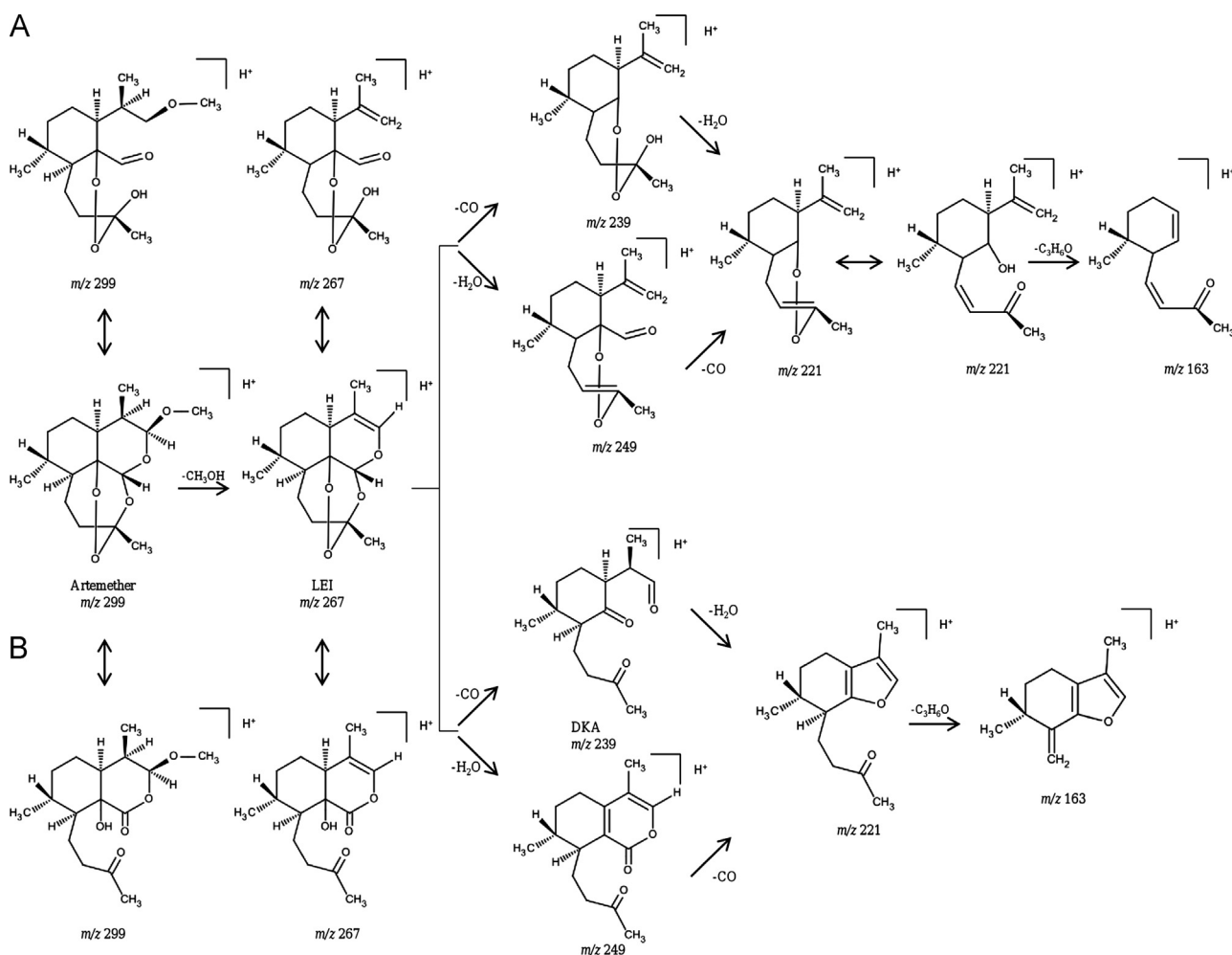
Fig. 6 Proposed fragmentation pattern of artemether, with the rupture of peroxide bridge as proposed in literature [48] (A), as currently proposed (B).

using the total area of the DHA epimers, our validation data showed that unwanted and variable on-column process did not significantly affect the reproducibility.

From the validation results (Table 3), it is concluded that the newly developed HPLC stability-indicating method is suitable for β-artemether assay in the 80–120% l.c. range, for DHA assay in the 2–6% range, and for other related substances (α-artemether and artemisinin) in the 0.1–0.3% l.c. range in paediatric powder for oral suspension.

The major improvement of the developed method lies within its selectivity, next to improved asymmetry factors and qualification limits, allowing notably the identification and quantification of β-artemether, but also of its related substances in bulky-excipients containing paediatric powders for stability studies, where excipients and other APIs will degrade as well.

The trioxane derivatives possess rather non-specific UV spectra, whereby the quantification of the β-artemether related degradation products is hampered by the absence of a selective UV-chromophor. Hence, false positive degradation peaks are a major problem in the HPLC stability-profiling of the FDP's. LC–MS analysis was considered to be very helpful: by using the typical ESI-mass spectra of the HPLC peaks, it was possible to confirm whether the HPLC-peak is a β-artemether related impurity in real-life samples. Our observation that MS detection is highly wanted, if not a requirement,

in the quality analysis of β-artemether and related trioxane drugs, is recently acknowledged by the USP-MC monographs containing β-artemether [54,55]. The observed m/z values are explained by proposed fragmentation patterns as given in Fig. 6 for β-artemether and Fig. 7 for artemisinin, respectively, and compared to those already described in literature [56–59].

The proposed fragmentation pathway of the cationized β-artemether (Li$^+$, Na$^+$ and K$^+$ -salt adducts) revealed by Dos Santos et al. [56] differs in the first fragmentation steps, i.e., they did not detect no significant signals for [AHA+H]$^+$ m/z 267 or [DKA+H]$^+$ m/z 239. This contrasts our observation, whereby m/z 267 and 239 are high intensity peaks, leading to the fragments with the similar characteristic m/z values of 221 and 163. Their hypothesis that artemether salt adducts undergo first isomerisation through the rupture of the peroxide ring [56] is not observed or supported by our data, as no observation was made of m/z 259 for Li$^+$-β-artemether salt adduct, which also corresponds with m/z-values of 254 for H$^+$, 271 for NH$_4^+$, 276 for Na$^+$ and 292 for K$^+$. Also the MS-spectra of the AHA and DKA-reference (see Supplementary information) (Table 4) give extra supportive information for structure elucidation of the β-artemether fragments by their characteristic m/z values. The parent ion of AHA [AHA+H]$^+$ with m/z 267 gives fragments with similar characteristics m/z values of 249, 239 [DKA+H]$^+$, 221 and 163, confirming the presence of
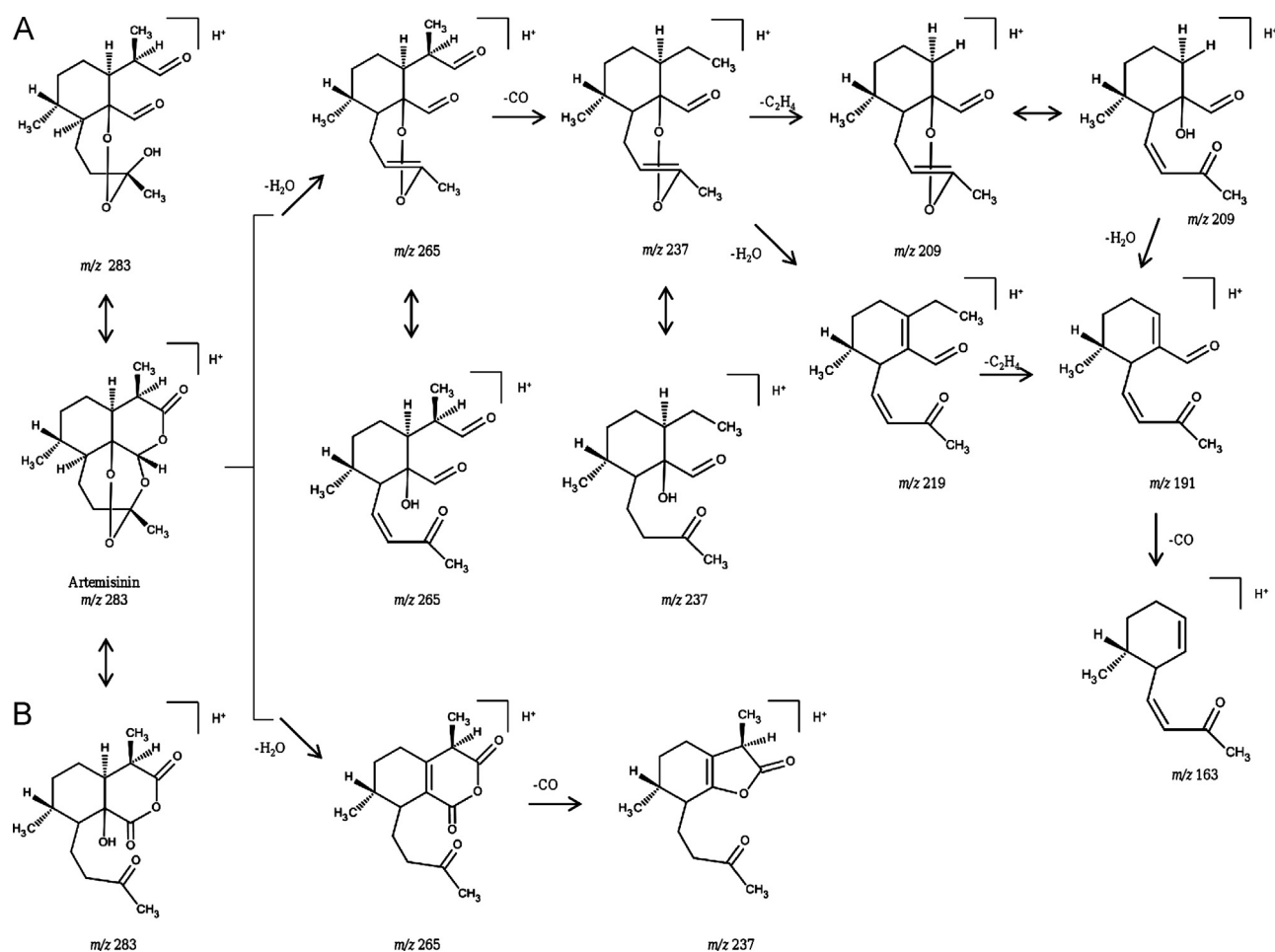
Fig. 7 Proposed fragmentation pattern of artemisinin, with the rupture of peroxide bridge as proposed in literature [48] (A), as currently proposed (B).

AHA in the MS-spectrum of β-artemether, meaning that the peroxide bridge is still present in the first fragmentation step. The differences in MS-spectra can be explained by differences between mobile phase composition, aqueous–organic ratio, adduct-ion type and concentration applied or present [60].

Moreover, α- and β-DHA with a m/z 285 corresponding to [DHA+H]$^+$ (Table 4), follow a similar fragmentation pattern, with dehydration (–H_2O) in the first step, leading to the same 9,10-anhydroartemisinin (AHA) m/z 267 and diketoaldehyde (DKA) m/z 239. DKA is also present as a related impurity in the DHA drug substance. Our findings are in line with the hypothetical fragmentation of DHA by Naik and co-workers [57]. Further elucidation of the fragmentation yielded m/z 163 [DHA+H–H_2O–CO–H_2O–C_3H_6O]$^+$ and m/z 145 [DHA+H–H_2O–CO–H_2O–C_3H_6O–H_2O]$^+$.

As mentioned in the previous section (see Section 3.3.2), artemisinin seems to follow another fragmentation pathway, different from β-artemether and its related derivatives (DHA, AHA and DKA). Artemisinin shows very characteristic m/z values of 283, 265, 237, 219 and 209. The product ion mass spectrum of artemisinin observed by Xing et al. [58] leads to their proposed fragmentation patterns of artemisinin and β-artemether (Figs. 6A and 7A). A variant structure for m/z 163 was proposed. Artemisinin differs only in its typical carbonyl group from the other artemisinin derivatives, whereby difference in the fragmentation between artemisinin and β-artemether can be explained by an altered carbocation stability of the fragments. The typical carbonyl group of artemisinin has a great influence on its fragmentation process, leading to a various protonation of the parent molecule during ESI-process and a various manner of peroxide bridge rupture [61].

Finally, there is no single characterstic m/z value, which can selectively identify the individual impurities. However, the combination of different m/z values can be used as qualifiers of β-artemether and its related (degradation) products. Using the characteristic in-source fragmentation, extracted ion or selected ion monitoring with the selected m/z values of 267, 239, 221 and 163 can thus be applied in complex mixtures, $e.g.$, paediatric powder for oral suspension, to collect or confirm the β-artemether relevant peaks. Using these settings, a real-life ICH-accelerated stability sample ($T_{6\ months}$; 40 °C/75% RH) could be evaluated for the peak assignments of the β-artemether degradation products.

5. Conclusions

This study reports for the first time a complete analytical characterisation of β-artemether and related compounds in a powder for oral suspension, which can be used for regulatory purposes. Volume effects are observed during the sample preparation of these paediatric formulations containing low API and high-bulk

excipient concentrations. Our results show that water is preferentially used up and/or adsorbed from the extraction solvent by pharmaceutical excipients, diminishing the freely available solvent and consequently increasing the apparent API concentration. The best extraction solvent for β-artemether and its related impurities was pure acetonitrile. Chromatography using a gradient elution on a Prevail OA column proved to be highly selective, and combined with appropriate sample preparation steps, this method can be employed for regulatory stability and quality control analysis. By adding MS analysis of the FPP, it was possible to acquire selective MS-data on the β-artemether degradants, whereby a fragmentation pathway of β-artemether, its related degradants and artemisinin is proposed.

Acknowledgments

Appendix A.   Supplementary materials

Supplementary data associated with this article can be found in the online version at http://dx.doi.org/10.1016/j.jpha.2013.03.006.

References

[1] Food & Drug Administration (FDA), Food and Drug Administration Amendments Act of 2007: Best Pharmaceuticals for Children Act. FDA, Silver Spring, 2007.

[2] European Medicine Evaluation Agency (EMEA), EMEA/CHMP/PEG/194810/2005: Reflection paper: formulations of choice for the paediatric population; EMEA, London, 2006.

[3] A. Ceci, C. Giaquinto, J.P. Aboulker, et al., The task-force in Europe for drug development for the Young (TEDDY) network of excellence, Paediatr. Drugs 11 (2009) 18–21.

[4] A. Zajicek, The national institutes of health and the best pharmaceuticals for children act, Paediatr. Drugs 11 (2009) 45–47.

[5] E. Connor, P. Cure, Creating hope and other incentives for drug development for children, Sci. Transl. Med. 3 (66) (2011) 66cm1.

[6] International Conference of Harmonisation (ICH), CPMP/ICH/2711/99 E11: Clinical Investigation of medical products in the paediatric population. EMEA, London, 2001.

[7] D.C. Knoppert, Paediatric formulations: international issues and potential solutions, Paediatr. Drugs 11 (2009) 55–56.

[8] World Health Organization (WHO), WHO/HTM/GMP/2008.1: World Malaria Report 2011, WHO Press, Geneva, 2011.

[9] J. Utzinger, M. Tanner, J. Keiser, ACTs for schistosomiasis: do they act? Lancet Infect. Dis. 10 (2010) 579–581.

[10] H.J. Li, W. Wang, Y.Z. Li, et al., Effects of artemether, artesunate and dihydroartemisinin administered orally at multiple doses or combination in treatment of mice infected with Schistosoma japonicum, Parasitol. Res. 109 (2011) 515–519.

[11] L. Rong, H.F. Dong, M.S. Jian, Artemisinin: the gifts from traditional Chinese medicine not only for malaria control but also for schistosomiasis control, Parasitol. Res. 110 (2012) 2071–2074.

[12] R. Sen, S. Ganguly, P. Saha, et al., Efficacy of artemisinin in experimental visceral leishmaniasis, Int. J. Antimicrob. Agents 36 (2010) 43–49.

[13] T. Efferth, M.R. Romero, D.G. Wolf, et al., The antiviral activities of artemisinin and artesunate, Clin. Infect. Dis. 47 (2008) 804–811.

[14] S. Chou, G. Marousek, S. Auerochs, et al., The unique antiviral activity of artesunate is broadly effective against human cytomegalovirus including therapy-resistant mutants, Antiviral Res. 92 (2011) 364–368.

[15] C. Zhang, L.B. Pei, L.L. Shi, et al., Anti-tumor effects of dihydroartemisinin on human osteosarcoma, Mol. Cell. Biochem. 351 (2011) 99–108.

[16] M.P. Crespo-Ortiz, M.Q. Wei, Antitumor activity of artemisinin and its derivatives: from a well-known antimalarial agent to a potential anticancer drug, J. Biomed. Biotechnol. 2012 (2012) 18, http://dx.doi.org/10.1155/2012/247597, Epub 2011 Nov 22.

[17] W. Aung, C. Sowaga, T. Furukawa, et al. Anticancer effect of dihydroartemisinin (DHA) in pancreatic tumor model evaluated by conventional methods and optical imaging, Anticancer Res. 31 (2011) 1549-1558.

[18] S. Soomro, T. Langenberg, A. Mahringer, et al., Design of novel artemisinin-like derivatives with cytotoxic and anti-angiogenic properties, J. Cell. Mol. Med. 15 (2011) 1122–1135.

[19] R.D. Slack, A.M. Jacobine, G.H. Posner, Antimalarial peroxides: advances in drug discovery and design, Med. Chem. Comm. 3 (2012) 281–297.

[20] C. Sungsik, O. Sangtae, U. Yumi, et al., Synthesis of 10-substituted triazolyl artemisinins possessing anticancer activity via huisgen 1,3-dipolar cycloaddition, Bioorg. Med. Chem. Lett. 19 (2009) 382–385.

[21] J. Chadwick, A.E. Mercer, B.K. Park, et al., Synthesis and biological evaluation of extraordinarily potent C-10 carba artemisinin dimers against P falciparum malaria parasites and HL-60 cancer cells, Bioorg. Med. Chem. 17 (2009) 1325–1338.

[22] H. Liu, Q. Li, S. Li, et al., The rapid determination of artemisinin by post-column derivatization high-performance liquid chromatography using matrix solid-phase dispersion method, J. Chromatogr. Sci. 46 (2008) 122–126.

[23] S. Liu, N. Tian, J. Li, et al., Simple and rapid micro-scale quantification of artemisinin in living Artemisia annua L. by improved gas chromatography with electron-capture detection, Biomed. Chromatogr. 23 (2009) 1101–1107.

[24] M. Quennoz, C. Bastian, X. Simonnet, et al., Quantification of the total amount of artemisinin in leaf samples by thin layer chromatography, Chimia 64 (2010) 755–757.

[25] K. Dost, G. Davidson, Analysis of artemisinin by a packed-column supercritical fluid chromatography-atmospheric pressure chemical ionisation mass spectrometry technique, Analyst 128 (2003) 1037–1042.

[26] C. Camps, M. Toussirot, M. Quennoz, et al., Determination of artemisinin and moisture content of Artemisinin annua L. dry powder using a hand-held near infrared spectroscopy device, J. Near Infrared Spec. 19 (2011) 191–198.

[27] M.K. Paudel, A. Takei, J. Sakoda, et al., Preparation of a single-chain variable fragment and a recombinant antigen-binding fragment against the anti-malarial drugs, artemisinin and artesunate, and their application in an ELISA, Anal. Chem. 84 (2012) 2002–2008.

[28] S.P. He, G.T. Tan, G. Li, et al., Development of a sensitive monoclonal antibody-based enzyme-linked immunosorbent assay for the antimalarial active ingredient artemisinin in the Chinese herb Artemisia annua L, Anal. Bioanal. Chem. 393 (2009) 1297–1303.

[29] U. Duthaler, J. Keiser, J. Huwyler, Development and validation of a liquid chromatography and ion spray tandem mass spectrometry method for the quantification of artesunate, artemether and their major metabolites dihydroartemisinin and dihydroartemisinin-glucuronide in sheep plasma, J. Mass Spectrom. 46 (2011) 172–181.

[30] J.F.S. Ferreira, J.M. Gonzalez, Analysis of underivatized artemisinin and related sesquiterpene lactones by high-performance liquid

chromatography with ultraviolet detection, Phytochem. Anal. 20 (2009) 91–97.

[31] C.S. Lai, N.K. Nair, A. Muniandy, et al., Validation of high performance liquid chromatography-electrochemical detection methods with simultaneous extraction procedure for the determination of artesunate, dihydroartemisinin, amodiaquine and desethylamodiaquine in human plasma for application in clinical pharmacological studies of artesunate-amodiaquine drug combination, J. Chromatogr. B. 877 (2009) 558–562.

[32] K. Gaudin, T. Kauss, A.M. Lagueny, et al., Determination of artesunate using reversed-phase HPLC at increased temperature and ELSD detection, J. Sep. Sci. 32 (2) (2009) 231–237.

[33] N. Lindegardh, W. Hanpithakpong, B. Kamanikom, et al., Quantification of dihydroartemisinin, artesunate and artemisinin in human blood: overcoming the technical challenge of protecting the peroxide bridge, Bioanalysis 3 (2011) 1613–1624.

[34] R. McGready, A.P. Phyo, M.J. Rijken, et al., Artesunate/dihydroartemisinin pharmacokinetics in acute *falciparum* malaria in pregnancy: absorption, bioavailability, disposition and disease effects, Clin. Pharmacol. 73 (2012) 467–477.

[35] N. Tian, J. Li, S.Q. Liu, et al., Simultaneous isolation of artemisinin and its precursors from *Artemisia annua* L. by preparative RP-HPLC, Biomed. Chromatogr. 26 (2012) 708–713.

[36] C. Ma, H. Wang, X. Lu, et al., Metabolic fingerprinting investigation of *Artemisia annua* L. in different stages of development by gas chromatography and gas chromatography-mass spectrometry, J. Chromatogr. A. 1186 (2008) 412–419.

[37] K.K. Jessing, N. Cedergreen, J. Jensen, et al., Degradation and ecotoxicity of the biomedical drug artemisinin in soil, Environ. Toxicol. Chem. 28 (2009) 701–710.

[38] K.K. Jessing, R.K. Juhler, B.W. Strobel, Monitoring of artemisinin, dihydroartemisinin, and artemether in environment matrices using high-performance liquid chromatography-tandem mass spectrometry (LC–MS/MS), J. Agric. Food Chem. 59 (2011) 11735–11743.

[39] I. Cesar, F.H.A. Nogueira, G. Pianetti, Simultaneous determination of artemether and lumefantrine in fixed dose combination tablets by HPLC with UV detection, J. Pharm. Biom. Anal. 48 (2008) 951–954.

[40] P.K. Saini, R.M. Singh, S.C. Mathur, et al., A simple and sensitive HPTLC method for quantitative analysis of artemether and lumefantrine in tablets, JPC J. Planar. Chromat. 23 (2010) 119–122.

[41] M.A. Atemnkeng, E. Marchand, J. Plaizier-Vercammen, Assay of artemether, methylparaben and propylparaben in a formulated paediatric antimalarial dry suspension, J. Pharmaceut. Biomed. 43 (2007) 727–732.

[42] S. Suleman, K. Vandercruyssen, E. Wynendaele, et al., A rapid stability-indicating fused core HPLC method for determination of β-artemether and lumefantrine in anti-malarial fixed dose combination products, Malaria J. 12 (2013), http://dx.doi.org/10.1186/1475-2875-12-145.

[43] R.W. Stringham, K.G. Lynam, P. Mrozinski, et al., High performance liquid chromatographic evaluation of artemisinin, raw material in the synthesis of artesunate and artemether, J. Chromatogr. A. 1216 (2009) 8919–8925.

[44] R.W. Stringham, M. Pennel, W. Cabri, et al., Identification of impurities in artemisinin, their behavior in high performance liquid chromatography and implications for the quality of derived anti-malarial drugs, J. Chromatogr A. 1218 (2011) 6836–6842.

[45] B.M.J. De Spiegeleer, M. D'Hondt, E. Vangheluwe, et al., Relative response factor determination of artemether degradants by a dry heat stress approach, J. Pharm. Biomed. Anal. 70 (2012) 111–116.

[46] International Pharmacopoeia (Int. Ph.). Specific monograph artemether injection. WHO, Genève, 2011.

[47] Software ACD/PhysChem suite [⟨http://www.acdlabs.com/products/pc_admet/physchem/physchemsuite/⟩] (accessed on 27 November at 19:10).

[48] M. Verbeken, S. Suleman, B. Baert, et al., Stability-indicating HPLC-DAD/UV-ESI/MS impurity profiling of the anti-malarial drug lumefantrine, Malaria J. (2011), http://dx.doi.org/10.1186/1475-2875-10-51.

[49] Y.L. Yeow, Y.K. Leong, Partial molar volumes of (acetonitrile+water) mixtures over the temperature range (273.15 to 318.15) K, J. Chem. Thermodyn. 39 (2007) 1675–1680.

[50] A. Gharsallaoui, B. Rogé, J. Génotelle, et al., Relationships between hydration number, water activity and density of aqueous sugar solutions, Food Chem. 106 (2008) 1443–1453.

[51] V.V. Mank, The improved chemical tracer technique for bound water determination, Colloid J. 64 (2002) 386–388.

[52] W. Cabri, I. D'Acquarica, P. Simone, et al., Stereolability of dihydroartemisinin, an antimalarial drug: a comprehensive thermodynamic investigation Part 1, J. Org. Chem. 76 (2011) 1751–1758.

[53] I. D'Acquarica, F. Gasparrini, D. Kotoni, et al., Stereodynamic investigation of labile stereogenic centres in dihydroartemisinin, Molecules 15 (2010) 1309–1323.

[54] Authorized Artemether USP MC Standard (September 2012). ⟨https://www.usp-mc.org/monographs/artemether-1-0⟩. (accessed on 27 November 2012 at 18:41).

[55] Authorized Artemether and Lumefantrine Tablets USP MC Standard (September 2012). [⟨https://www.usp-mc.org/monographs/artemether-and-lumefantrine-tablets-1-0⟩]. (accessed on 27 November 2012 at 18:43).

[56] V.G. Dos Santos, J.R. Alves, M.N. Eberlin, et al., Electrospray ionization tandem mass spectrometry of the two main antimalarial drugs: artemether and lumefantrine, J. Braz. Chem. Soc. 23 (2012) 65–71.

[57] H. Naik, D.J. Murry, L.E. Kirsh, et al., Development and validation of high-performance liquid chromatography-mass spectroscopy assay for determination of artesunate and dihydroartemisinin in human plasma, J. Chromatogr. B 816 (2005) 233–242.

[58] J. Xing, H. Yan, S. Zhang, et al., A high-performance liquid chromatography/tandem mass spectrometry method for the determination of artemisinin in rat plasma, Rapid Commun. Mass Spectrom. 20 (2006) 1463–1468.

[59] C. Souppart, N. Gauducheau, N. Sandrenan, et al., Development and validation of a high-performance liquid chromatography-mass spectrometry assay for determination of artemether and its metabolite dihydroartemisinin in human plasma, J. Chromatogr. B 774 (2002) 195–203.

[60] J. Wang, A. Aubry, M.S. Bolgar, et al., Effect of mobile phase pH, aqueous-organic ratio, and buffer concentration on electrospray ionization tandem mass spectrometric fragmentation patters: implications in liquid chromatography/tandem mass spectrometric bioanalysis, Rapid Commun. Mass Spectrom. 24 (2010) 3221–3229.

[61] L. Dhooghe, S. Van Miert, H. Jansen, et al., A new decomposition product of dihydroartemisinin, Pharmazie 62 (2007) 900–901.

[62] A.E.M. Crotti, T. Fonseca, H. Hong, et al., The fragmentation mechanism of five-membered lactones by electrospray ionisation tandem mass spectrometry, Int. J. Mass. Spectrom. 232 (2004) 271–276.

[63] R.K. Haynes, H.W. Chan, M.K. Cheung, et al., C-10 ester and ether derivatives of dihydroartemisinin – 10-alpha artesunate, preparation of authentic 10-beta artesunate, and of other ester and ether derivatives bearing potential aromatic intercalating groups at C-10, Eur. J. Org. Chem. 1 (2002) 113–132.

[64] Authorized USP Salmous Artemether Standard (February 2009). ⟨http://www.usp.org/sites/default/files/usp_pdf/EN/nonUSStandards/artemether.pdf⟩ (accessed on 27 November 2012 at 18:52).

[65] International Pharmacopoeia, Fourth Edition, 2011. Specified monograph of dosage form Artemether and Lumefantrine Tablets. ⟨http://apps.who.int/phint/en/p/docf/⟩ (accessed on 27 November 2012 at 18:50).

[66] J.N. Lisgarten, B.S. Potter, C. Bantuzeko, et al., Structure, absolute configuration, and confirmation of the antimalarial compound, artemisinin, J. Chem. Crystallograph. 28 (1998) 539–543.

[67] R.J. Butcher, J.P. Jasinski, H.S. Yathirajan, et al., Alpha artemether, Acta Crystallograph. E. 63 (2007) O3291–U4212.

[68] R.K. Haynes, C.M. Ho-Wai, C.M. Lung, et al., Artesunate and dihydroartemisinin (DHA): unusual decomposition products formed under mild conditions and comments the fitness of DHA as an antimalarial drug, ChemMedChem. 2 (2007) 1448–1463.

[69] S.R. Meshnick, T.E. Taylor, S. Kamchonwongpaisan, Artemisinin and the antimalarial endoperoxides: form herbal remedy to targeted chemotherapy, Microbiol. Rev. 60 (1996) 301–315.

[70] P. Christen, J.L. Veuthey, New trends in extraction, identification and quantification of artemisinin and its derivates, Curr. Med. Chem. 8 (2001) 1827–1839.

[71] H.J. Woerdenbag, N. Pras, R. Bos, et al., Analysis of artemisinin and related sesquiterpenoids from Artemisia-annua L by combined gas-chromatography mass-spectrometry, Phytochem. Anal. 2 (1991) 215–219.

[72] B. Yagen, Y.M. Pu, H.J.C Yeh, et al., Tandem silica gel-catalyzed rearrangements and subsequent Baeyer–villiger reactions of artemisinin derivates, J. Chem. Soc. Perkin. Trans. 7 (1994) 843–846.

[73] F.C.W Van Nieuwerburgh, S.R.F Vande Casteele, L. Maes, et al., Quantitation of artemisinin and its biosynthetic precursors in Artemisia annua L. by high performance liquid chromatography-electrospray quadurpole time-of-flight tandem mass spectrometry, J. Chromatogr. A 1118 (2006) 180–187.